

# **STRENGTH PROPERTIES OF ROCKS AND ROCK MASSES**

## **1. INTRODUCTION**

## **2. TESTING OF INTACT ROCK FOR STRENGTH**

- 2.1 Uniaxial Compression
- 2.2 Point Load Testing
- 2.3 Uniaxial Tension
- 2.4 Indirect Tension Tests
- 2.5 Shear Tests
- 2.6 Confined Compression Tests (Triaxial Tests)
- 2.7 Biaxial and Multiaxial Tests
- 2.8 Other Tests

## **3. PARAMETERS AFFECTING ROCK STRENGTH**

## **4. FAILURE CRITERIA FOR INTACT ROCKS AND ROCK MASSES**

- 4.1 Mohr Criterion
- 4.2 Mohr-Coulomb Criterion
- 4.3 Hoek and Brown Criterion
- 4.3 Other Criteria

## **5. REFERENCES**

## 1. INTRODUCTION

For civil and mining engineering projects that involve rocks either as construction or foundation materials, a question which often arises in practice is: "will the combination of initial stresses and stresses induced by the construction and operation of an engineering structure produce rock failure and what will be the extent of the failure zone". In order to answer that question, it is necessary to know how the stresses are redistributed due to the rock-structure interaction and what is the rock mass strength. Knowledge of rock mass strength is also important in the design of support systems as discussed in the next set of notes with regard to the concept of rock-support interaction.

In general, rock mass strength depends on the strength of intact rock and the strength of rock discontinuities. In general, compared to intact rock, a rock mass has reduced tensile strength (almost zero), and reduced shear strength especially along discontinuity planes. Furthermore, if a rock mass is cut by directional joint sets, the rock mass strength is anisotropic. Rock mass strength is scale dependent and varies with the volume of rock under consideration.

The modes of failure of intact rock are multiple. Rock can fail in tension, compression or shear. This depends on the load configuration, the geometry of the problem and how the loads are applied and distributed. A rock mass can also fail in tension, compression or shear. However, the failure may involve the intact rock only, the discontinuities only, or may be mixed and involve both the intact rock and the discontinuities.

## 2. TESTING OF INTACT ROCK FOR STRENGTH

### 2.1 Uniaxial Compression

Recall the typical stress strain response curve for a specimen of intact rock under uniaxial compression (see Figure 1 in Lecture Notes 5). Part OA represents the closing of existing cracks in the rock and an overall readjustment of the rock testing machine setup whereas part AB represents the elastic rock response. Using AE (acoustic emission) devices, it has been found that starting at point B microcracks develop in the rock sample and the sample experiences strain hardening. The ordinate of point B is called the *yield stress* by analogy with the response of concrete samples. The maximum ordinate of the curve (Point C) that marks the transition between strain hardening and softening is called the *unconfined compressive strength* of the rock and is denoted as  $C_o$  or  $q_u$ . Failure takes place continuously from C to D during which macrocracking takes place as the rock becomes more deteriorated and crack coalescence takes place.

Various authors have compiled the values of the unconfined compressive strength for different rock types (Balmer, 1953; Johnson and DeGraff, 1988; Hatheway and Kiersch, 1989; Goodman, 1989; etc.). Typical values are given in Tables 1 and 2.

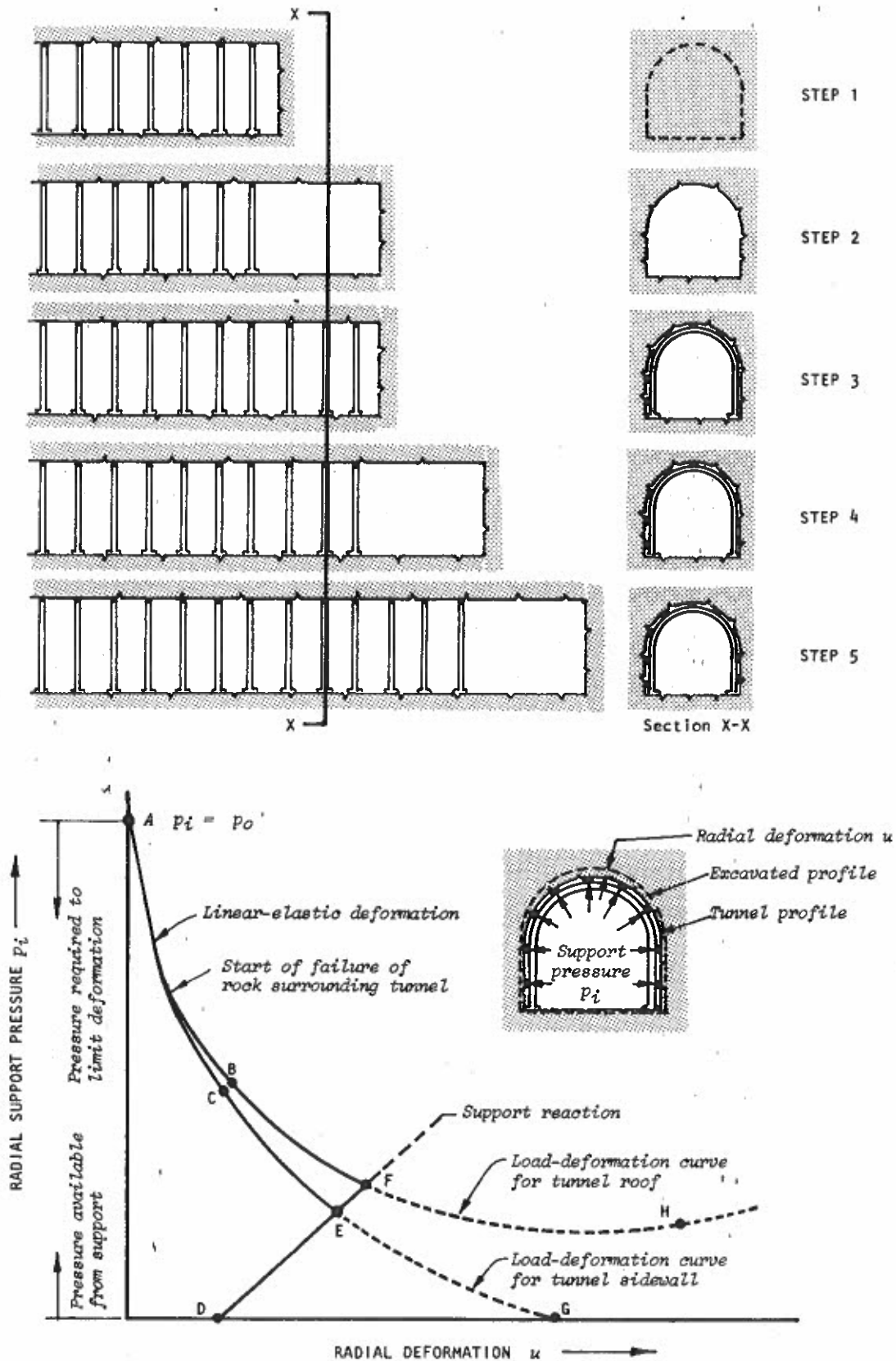


Figure 129 : Hypothetical example of a tunnel being advanced by full face drill and blast methods with blocked steel sets being installed after each mucking cycle. The load-deformation curves for the rock mass and the support system are given in the lower part of the figure. (After Daeman<sup>224</sup>).

	Granite	Basalt	Gneiss	Schist	Quartzite	Marble	Limestone	Sandstone	Shale
Av. C <sub>o</sub>	181.7	214.1	174.4	57.8	288.8	120.5	120.9	90.1	103.0
Max. C <sub>o</sub>	324.0	358.6	251.0	165.6	359.0	227.6	373.0	235.2	231.0
Min. C <sub>o</sub>	48.8	104.8	84.5	8.0	214.9	62.0	35.3	10.0	34.3
Range	275.2	253.8	166.5	157.6	144.1	165.5	337.7	225.2	196.7
No. of samples	26	16	24	17	7	9	51	46	14

Table 1. Typical values of uniaxial strength (in MPa) for nine common rock types (after Johnson and Degraff, 1988).

Rock	Tensile Strength (MPa)	Compressive Strength (MPa)
Limestone	18.00 ± 0.62 (20)	41.45 ± 3.52 (4)
Sandstone	19.17 ± 0.21 (23)	77.59 ± 1.59 (5)
Sandstone	23.10 ± 0.48 (19)	80.83 ± 2.21 (10)
Sandstone	24.21 ± 0.83 (8)	90.48 ± 3.86 (4)
Mudstone	35.17 ± 3.17 (4)	50.07 ± 3.79 (4)
Limestone	36.28 ± 1.24 (24)	142.55 ± 6.14 (5)
Limestone	38.76 ± 2.69 (23)	142.97 ± 19.10 (8)
Ironstone	44.28 ± 4.48 (5)	190.69 ± 17.93 (4)
Sandstone	65.66 ± 0.83 (11)	167.66 ± 9.86 (5)

Table 2. Mean tensile strength and compressive strength for selected sedimentary rock types (after Johnson and Degraff, 1988).

The behavior of intact rock in the post-peak domain is not a true rock property and is partially dependent on the stiffness of the loading system. A testing machine consists of an assembly of cross heads, tie bars, platens, screws and hydraulic cylinders, pipes and hydraulic oil contributing on their own to the total machine stiffness. By using stiff testing machines (low energy stored), or more recently servo-controlled testing machines, it is possible to observe the post-peak response of rocks (Hudson et al., 1971). Otherwise, for soft machines (high energy stored) sudden failure may take place at point C. In the field, the stiffness of the testing machine is replaced by the stiffness of the rock mass surrounding the volume of rock of interest.

Uniaxial compression tests require a careful test set-up and strict specimen preparation. Requirements for specimen preparation and testing are discussed in ASTM D-2938-86 and in the ISRM suggested methods (Bieniawski and Bernede, 1979). End effects can also be important

especially if the load platens are not chosen accordingly. End platens can create lateral restraint and a stress state far from being uniaxial. Lubricants can also be used such as teflon. However their effectiveness has been put in doubt at several occasions since they can initiate longitudinal splitting. The ideal platens would be made out of a medium that has same lateral expansion as the rock being tested.

## 2.2 Point Load Testing

In order to overcome many of the problems associated with the unconfined compression test, Broch and Franklin (1972) proposed a testing method called the *Point Load Test*. The test consists of squeezing pieces of rock diametrically between two hardened steel cones. The test set-up is shown in Figure 1. For these tests, rock pieces must have a length at least 1.4 times their diameter (Figure 2a). The *point load index*,  $I_p$ , is equal to

$$I_p = P/D^2 \quad (1)$$

where P is the load at rupture and D is the core diameter. Rock specimens break since tensile cracks develop parallel to the loading direction. In general, it has been found that the value of the load P at failure depends largely on the core diameter. Hence, the results of point load tests are usually presented in terms of a reference diameter equal to 50 mm. If the diameter is not equal to 50 mm, a correction is required (Figure 3). The unconfined compressive strength  $q_u$  is related to the point load index with 50 mm cores  $I_{p,50}$  as follows

$$q_u = 24 I_{p,50} \quad (2)$$

Beside the diametral test, the axial test and the irregular lump test have also been proposed (see Figures 2b and 2c). Strength anisotropy can also be assessed by using the point load index as suggested by Broch (1983) who proposed an *anisotropy index*  $I_a$  equal to

$$I_a = I_{p1}/I_{p2} \quad (3)$$

## 2.3 Uniaxial Tension

Direct measurements of tensile strength are difficult. Gripping systems or the use of cement at the test specimen ends can produce unwanted stress concentrations and create premature failure. More recently, strong structural epoxies are available to carry out uniaxial tension tests. The testing procedure is described in ASTM D 2936-84 and in Bieniawski and Hawkes (1978).

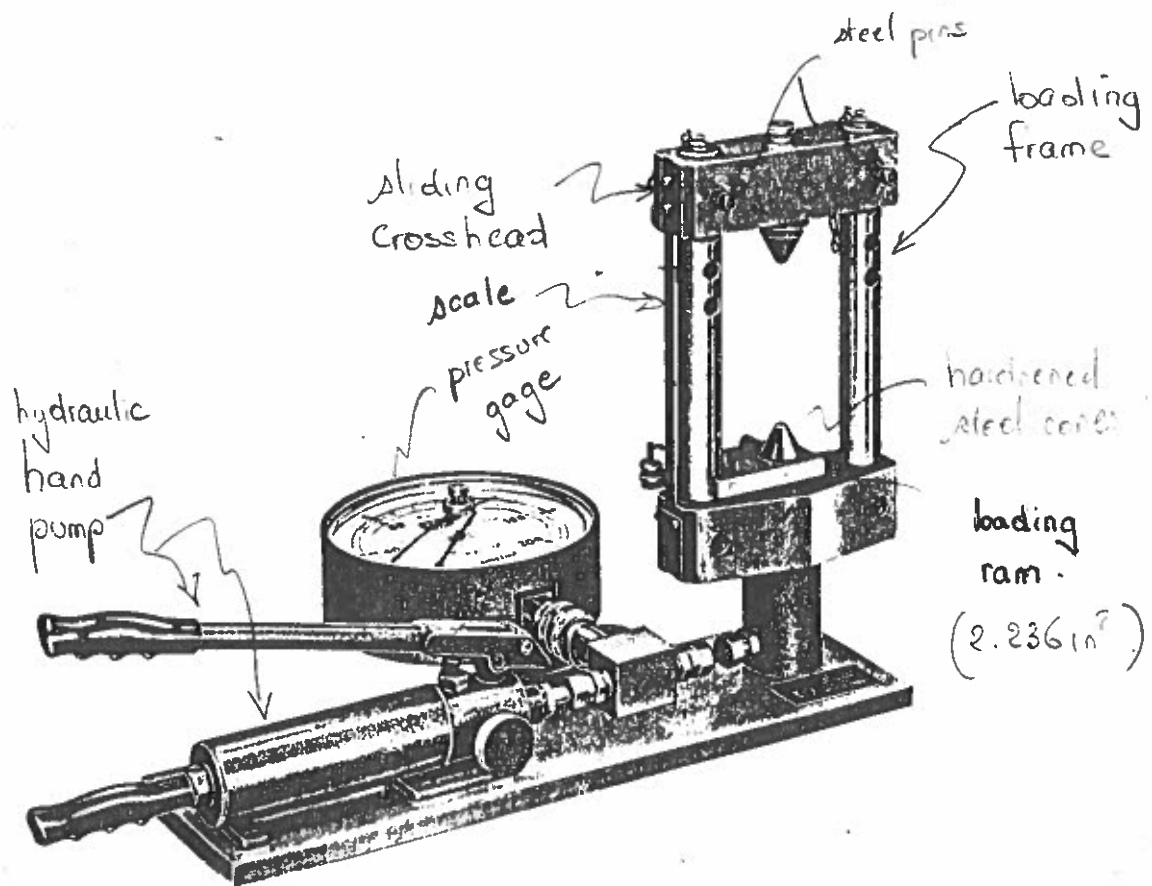


Figure 1. Point load testing equipment.

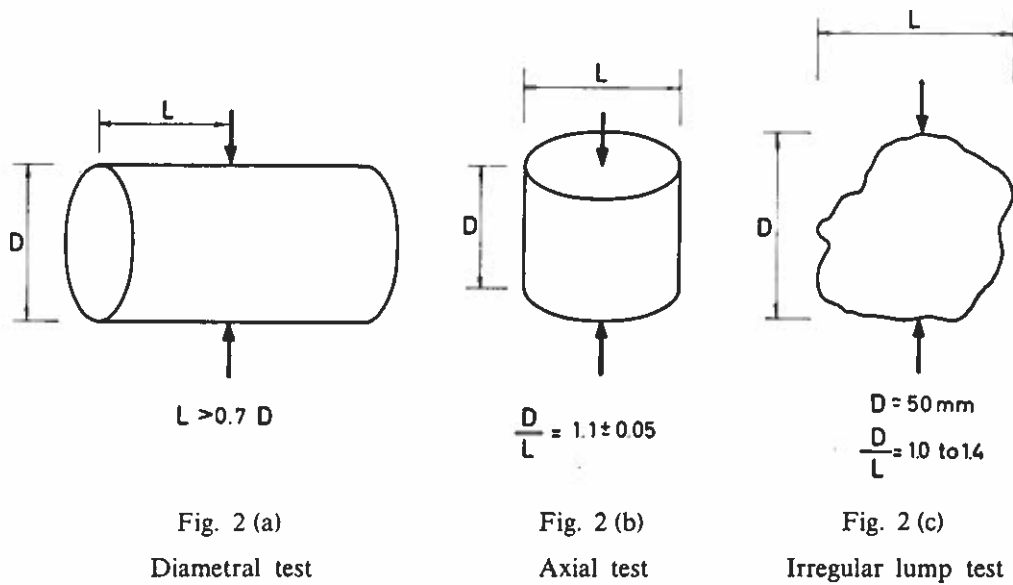


Figure 2. Types of point load tests.

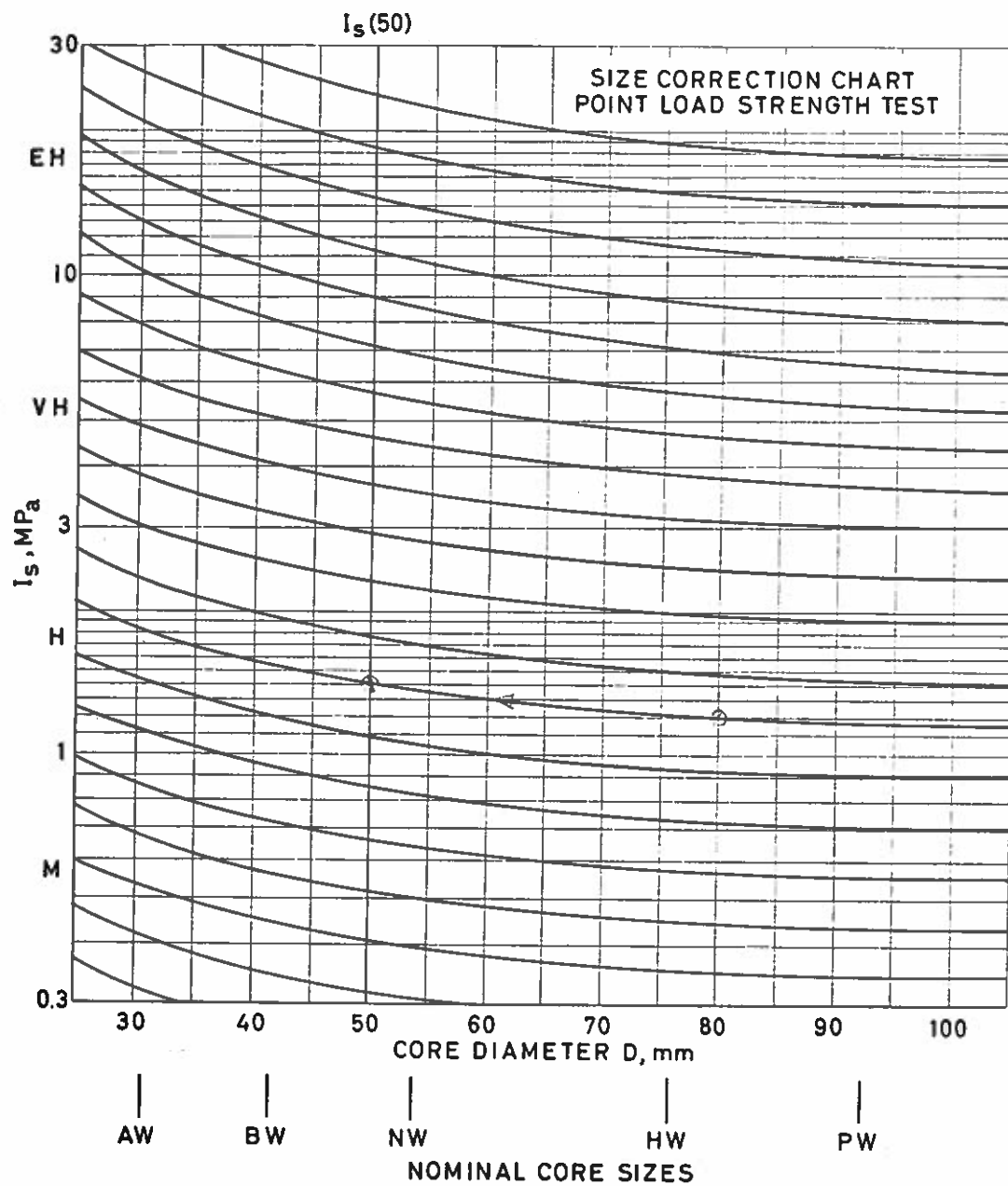


Figure 3. Chart used for diameter correction.

## 2.4 Indirect Tension Tests

Difficulties associated with performing direct uniaxial tension tests have led to a number of indirect methods such as the splitting tension test (also called Brazilian or diametral compression test) and the flexural tests.

### *The Brazilian Test*

The test consists of applying diametral compression to induce tensile stresses in a thin disc of rock. As shown in Figure 4a, a line load creates a uniform tensile stress across the loaded diameter accompanied with a vertical compressive stress. Failure is assumed to start at the center under a state of stress

$$\sigma_1 = \frac{6P}{\pi Dt} ; \quad \sigma_2 = 0 ; \quad \sigma_3 = -\frac{2P}{\pi Dt} \quad (4)$$

where P is the applied load, D is the core diameter and t the core thickness. Equation (4) can only be used if the rock is isotropic. If the rock is anisotropic, equation (4) is replaced by equation (28) in Lecture Notes 5.

When using the Brazilian test to determine the indirect tensile strength of rock, it is usually assumed that failure is the result of the uniform tensile stress normal to the splitting diameter (see Figure 4a) and that the tensile strength,  $T_o$ , is given by the value of  $\sigma_3$  ( $= -T_o$ ) at failure

$$T_o = \frac{2P}{\pi Dt} \quad (5)$$

Special precautions must be taken at the contact between the rock and the loading platens to avoid crushing that could throw doubts as to the mechanism of failure in the test sample. Strips of paper or steel loading jaws (Figure 4c) are often used to replace the point load by a strip load over an angle not exceeding  $10^\circ$  (Figure 4b). It can be shown that the stress distribution is only affected near the surface contacts but not in the body of the disc specimens, and in particular at their center.

### *Flexural Tests*

Flexural tests are conducted by bending cylindrical or prismatic rock beams. Three point or four point flexural loading tests can be conducted. For the geometry shown in Figures 5a and 5b, the flexural strength (sometimes called the modulus of rupture) is calculated as the maximum tensile stress existing on the lower fiber of the beam at peak load. Using simple beam theory and three

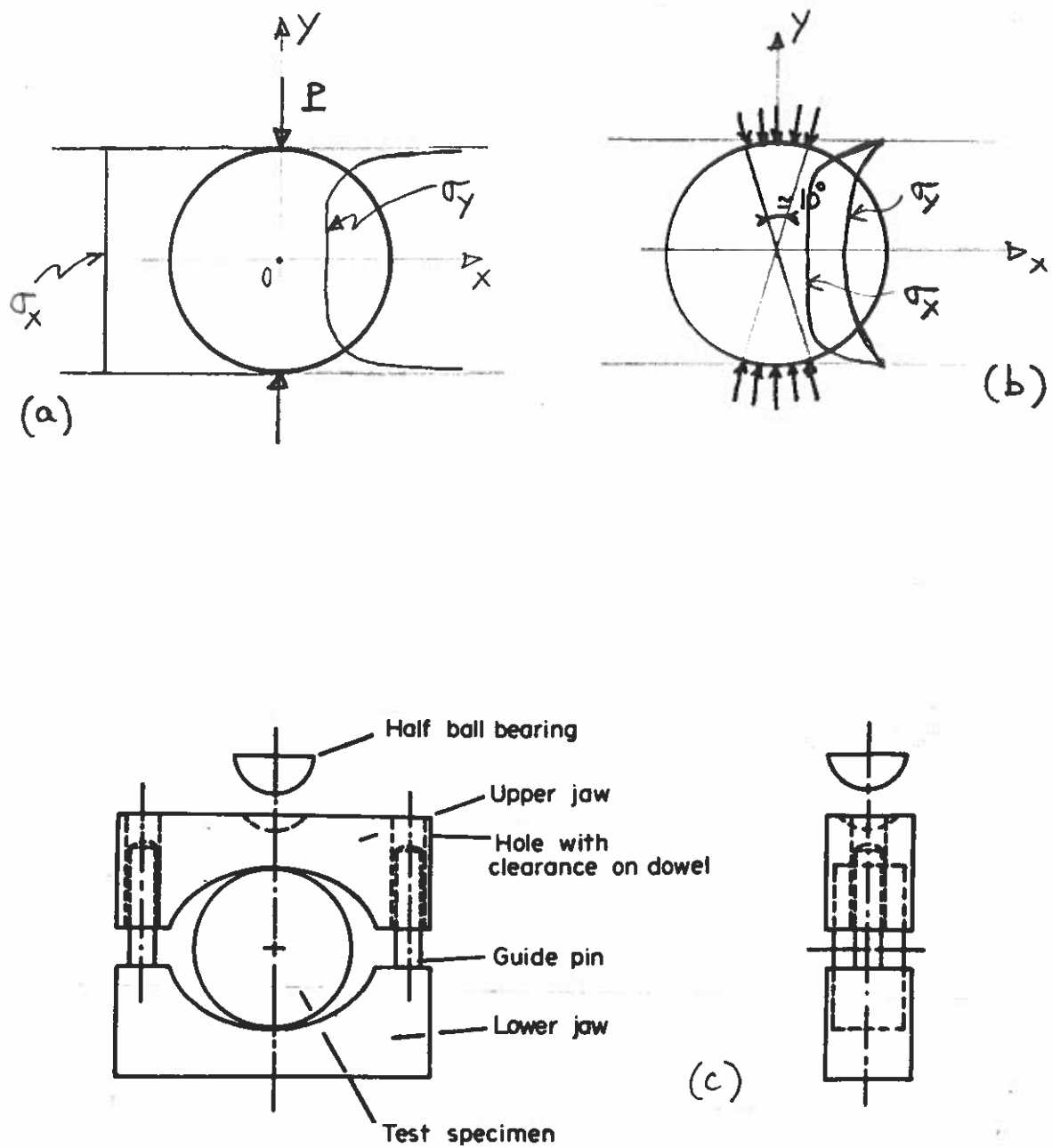


Figure 4. Stress distribution in a disc of rock under diametral compression. (a) Line load, (b) Strip load, (c) Steel loading jaws recommended by the ISRM.

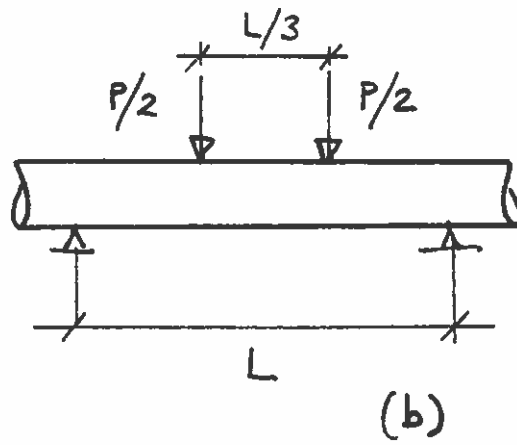
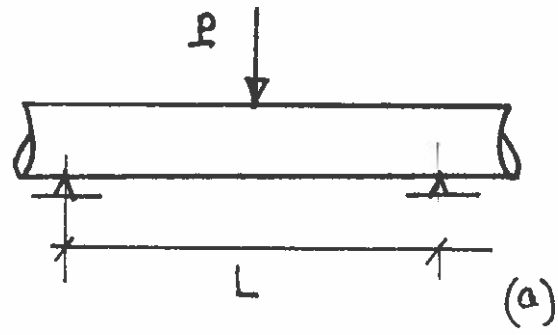


Figure 5. Flexural test set-up. (a) Three point loading, (b) Four point loading.

point loading (Figure 5a), the tensile strength is equal to

$$T_o = \frac{8PL}{\pi D^3} \quad (6)$$

and

$$T_o = \frac{3PL}{2ba^2} \quad (7)$$

for cylindrical and prismatic specimens respectively. In equations (6) and (7), P is the maximum applied load, L the length between supports, D the specimen diameter, a is the beam thickness and, b, is its width. For four point loading (Figure 5b), equation (6) is replaced by the following

$$T_o = \frac{16PL}{3\pi D^3} \quad (8)$$

Note that in general, the tensile strength measured using the indirect methods is less than that measured using a direct tension apparatus.

## 2.5 Shear Tests

Direct simple, double or punch shear tests can be conducted on rock. The tests allow a direct measurement of the intact rock shear strength. However, they are difficult to perform.

## 2.6 Confined Compression Tests (Triaxial Tests)

Confined compression tests can be conducted using a confining vessel similar to the one used for measuring the strength of soils. The so-called *Hoek cell* is often used in this test. Figure 6a shows the original Hoek cell and Figure 6b is a modified confining cell developed at the University of Colorado at Boulder. Two series of tests can be conducted with such devices: (i) triaxial compression tests  $\sigma_1, \sigma_2 = \sigma_3$ , and, (ii) triaxial extension tests  $\sigma_1 = \sigma_2, \sigma_3$ . Triaxial tests have been conducted on cylindrical specimens, shaped specimens (dog bone specimens) and hollow cylinders (Jaeger and Cook, 1976).

## 2.7 Biaxial and Multiaxial Tests

The Hoek cell cannot be used for the testing of rocks under true biaxial and triaxial loading conditions. Such stress states exist in rock masses. Biaxial tests have been conducted by various authors. Among them, Brown (1974) studied the biaxial compressive strength of Wombeyan

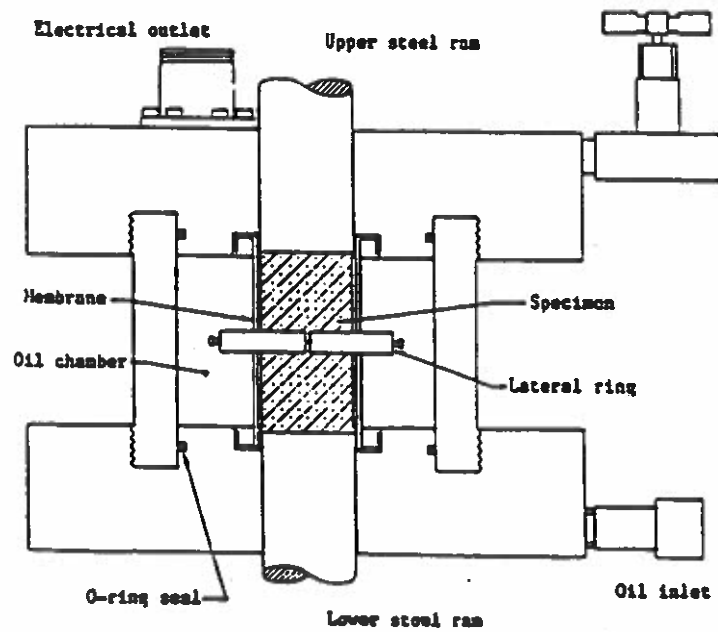
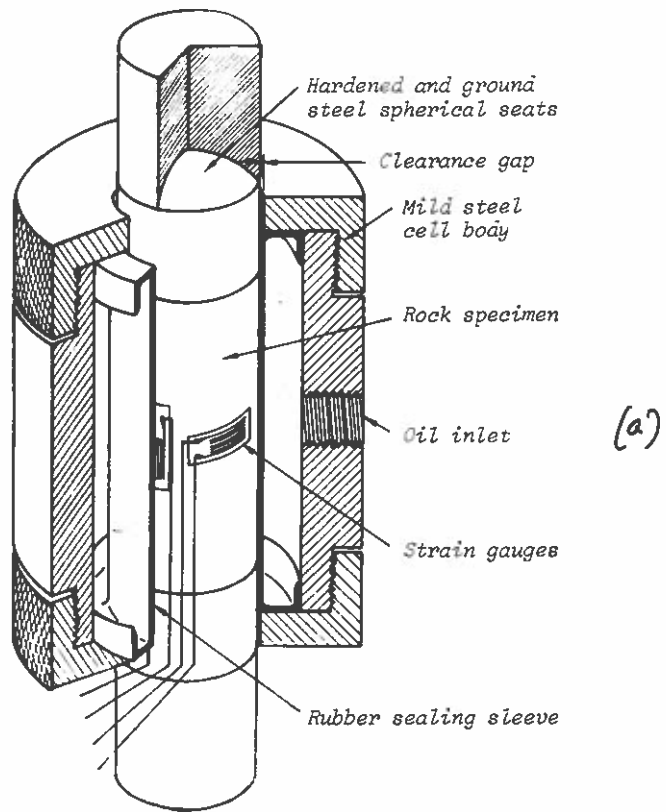


Figure 6. Hoek cell and modified Hoek cell.

marble by testing prismatic specimens. In his research, Brown emphasized the role played by the loading platens (end effects) on the rock strength (Figures 7a and 7b); different strengths can be obtained with different platens.

True triaxial apparatuses are limited. Mogi (1971) developed such an apparatus and reported the results of multiaxial triaxial tests on dolomite and limestone. A large amount of true triaxial tests have been conducted at the University of Colorado at Boulder using a *cubical cell* developed by Sture (1973). The cell can be used to determine the deformability and strength of 4 in. cubical specimens under a wide range of states of stress. The compression on each face of a test specimen is applied using a compressive loading system such as that shown in Figure 8a. Each compressive loading system can also be replaced by a tensile loading system (Figure 8b) thus allowing for various combinations of tensile stress regimes, and mixed compressive tensile stress regimes. Since 1973, the cubical cell has been updated and has been used for the testing of various geomaterials such as rock, concrete, and soils. Results of an extensive testing program (102 tests) on Indiana limestone can be found in the MS thesis of Robison (1985).

## **2.8 Other Tests**

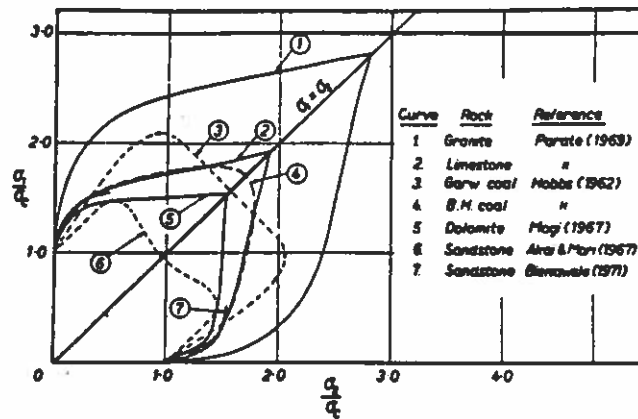
Other tests are also available for the testing of rock. These include:

- hollow cylinder tests,
- fracture toughness tests (fracture mechanics),
- punching tests, and,
- torsional tests.

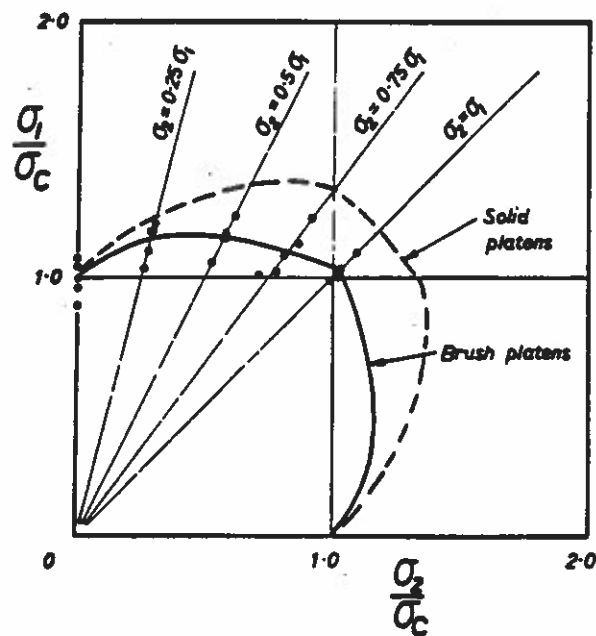
## **3. PARAMETERS AFFECTING ROCK STRENGTH**

Rock strength depends on many parameters (Paterson, 1978) including:

- rock type and composition,
- rock grain size,
- rock weathering,
- rock density and porosity,
- rate of loading,
- confining stresses  $\sigma_2$  and  $\sigma_3$ ,
- geometry, size and shape of the test specimens,
- rock anisotropy,
- water pore pressure and saturation,
- testing apparatus (end effects, stiffness),
- temperature, and,
- time.



(a)



(b)

Figure 7. (a) Biaxial failure envelopes obtained by various researchers, (b) biaxial failure envelopes for Wombeyan marble (after Brown, 1974).

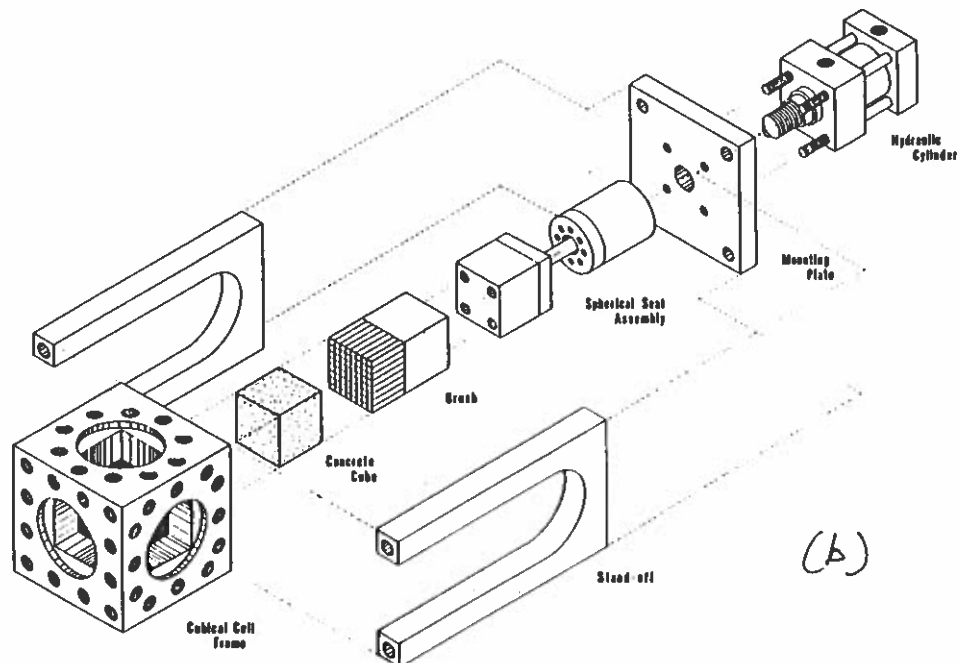
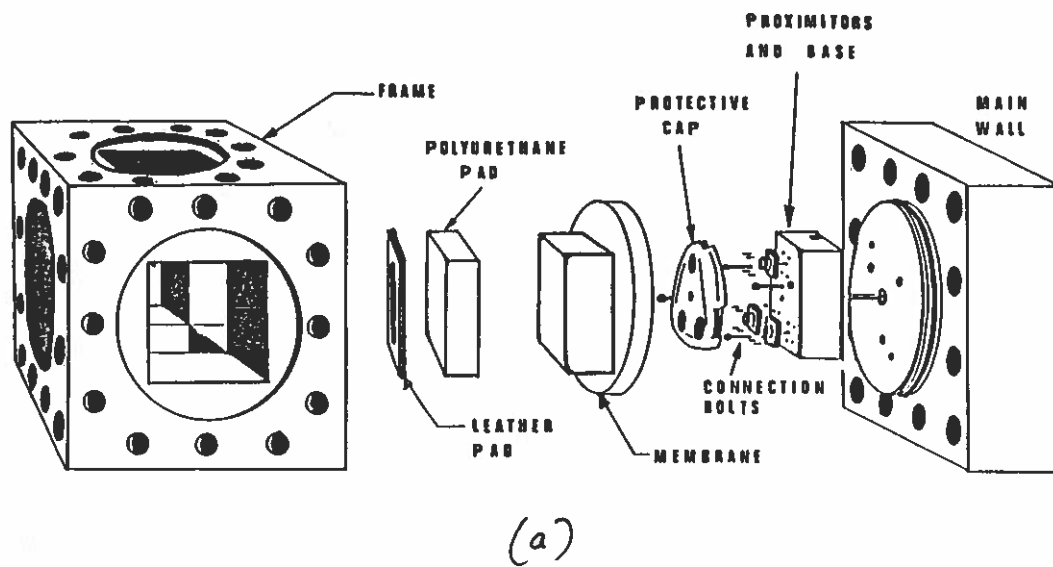


Figure 8. True triaxial equipment (cubical cell) available at CU Boulder. (a) compressive loading system, (b) tensile loading system.

The following trends have been observed:

- (1) a finer rock grain size leads to higher fracture strengths.
- (2) strength decreases with the size of the test specimen (Figure 9).
- (3) confinement increases strength. The effect of the intermediate stress is not consistent for all rocks. For confined compression tests, increasing  $\sigma_3$  may lead to a transition from brittle to ductile behavior. The pressure at the transition is high for igneous and metamorphic rocks. On the other hand for carbonate and evaporite rocks and clay bearing rocks, the transition occurs at lower confining stress values. According to Mogi (1966), rocks show a brittle behavior as long as  $\sigma_3$  is less than  $\sigma_1/3.4$ . Loading of rocks in hydrostatic compression does not show any peak load response. Figure 10 shows the results of true triaxial tests conducted by Mogi (1971).
- (4) rock anisotropy may lead to high strength anisotropy.
- (5) igneous and high grade metamorphic rocks show unconfined compressive strengths ranging between 100 and 200 MPa. Low porosity and low to medium grade metamorphic rocks show unconfined compressive strengths ranging between 50 and 100 MPa. High porosity and some low grade metamorphic rocks show unconfined compressive strengths ranging between 10 and 50 MPa. Low porosity dolomite and quartzite can have unconfined compressive strengths up to 300 MPa.
- (6) uniaxial tensile strengths are usually 10 to 20 times lower than unconfined compressive strengths.
- (7) end effects can have a large effect on rock strength. The test specimens must be large enough to reduce that effect.
- (8) fracture strength decreases as temperature increases (see Lecture Notes 4).
- (9) fracture type depends on the stress conditions (see Figure 11).
- (10) fracture strength decreases as porosity increases.
- (11) Strength can decrease with time due to stress corrosion effects. This phenomenon has been observed for igneous rocks (stress fracture).
- (12) Clay bearing rocks are very sensitive to water due to weathering and slaking. Strength decreases as the weathering increases. For rocks that do not disintegrate, saturated strength is usually less than the oven dried strength. This can be explained by using the effective stress concept proposed by Terzaghi.

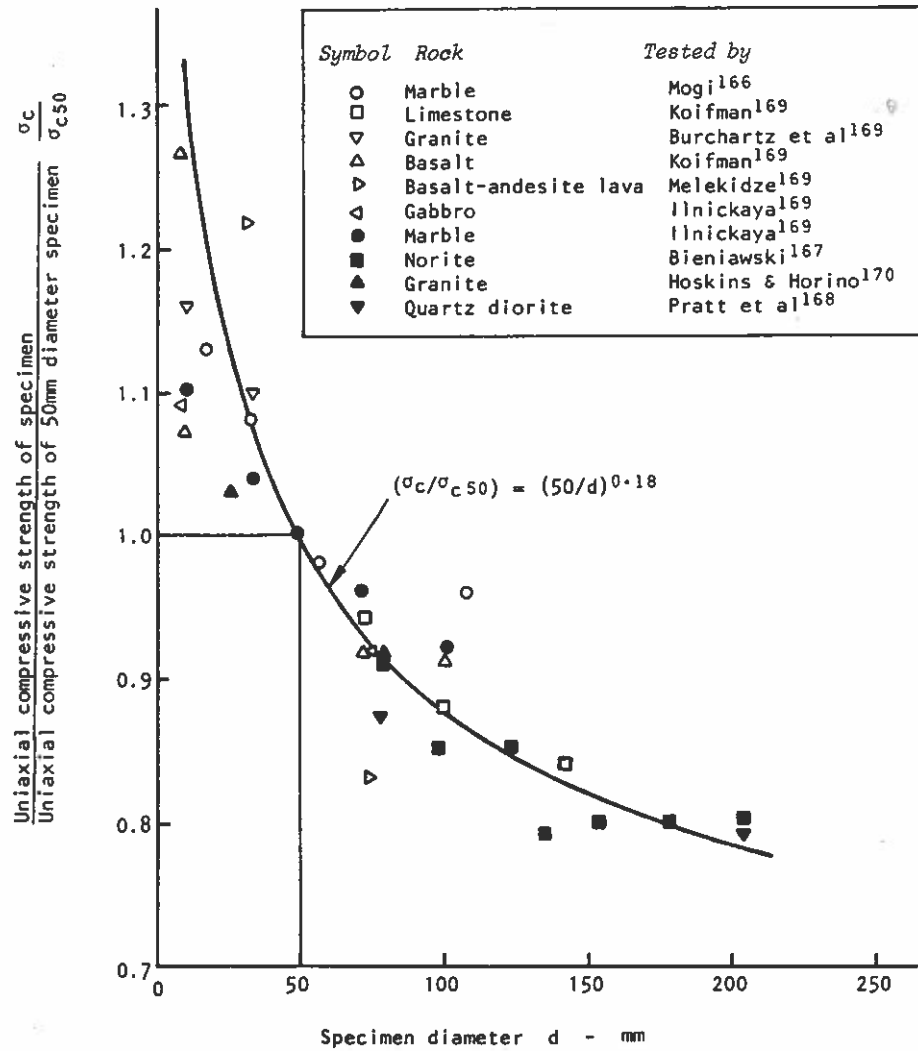


Figure 9. Influence of specimen size on the strength of intact rock (after Hoek and Brown, 1980a).

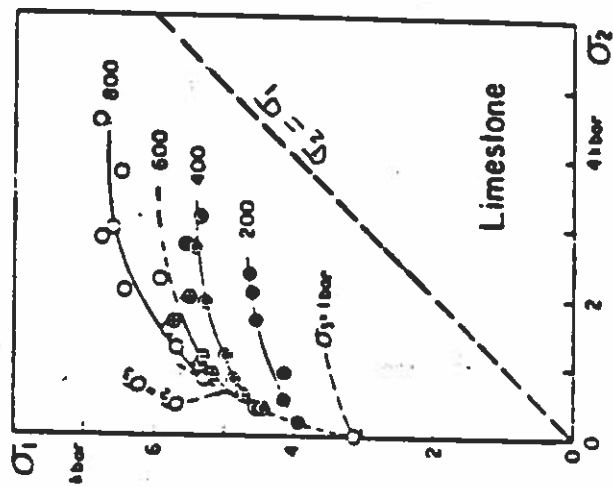
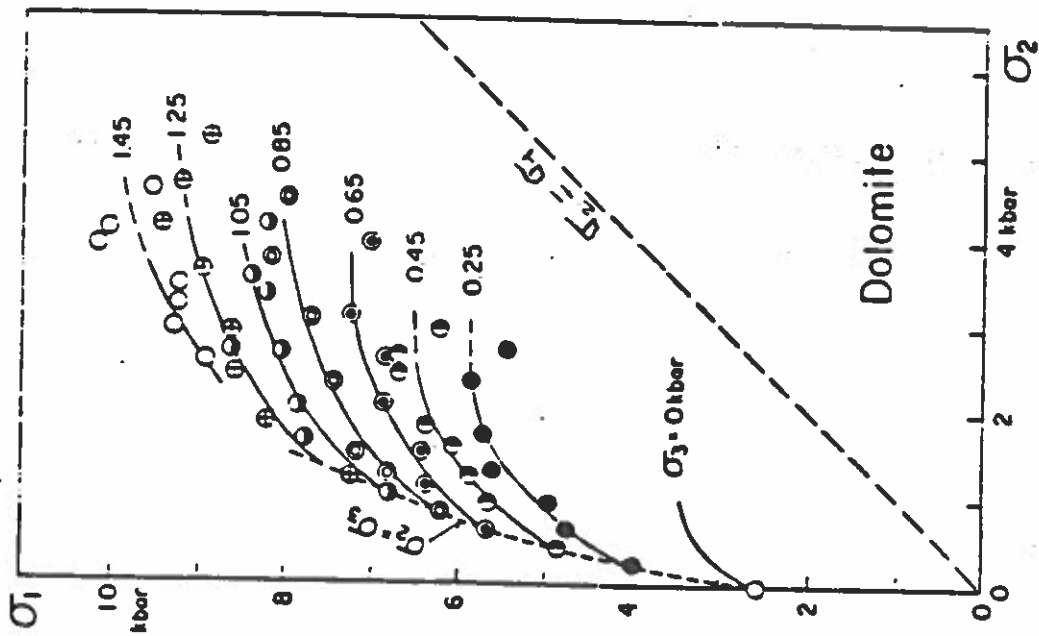


Figure 10. Biaxial and triaxial test results (after Mogi, 1971).

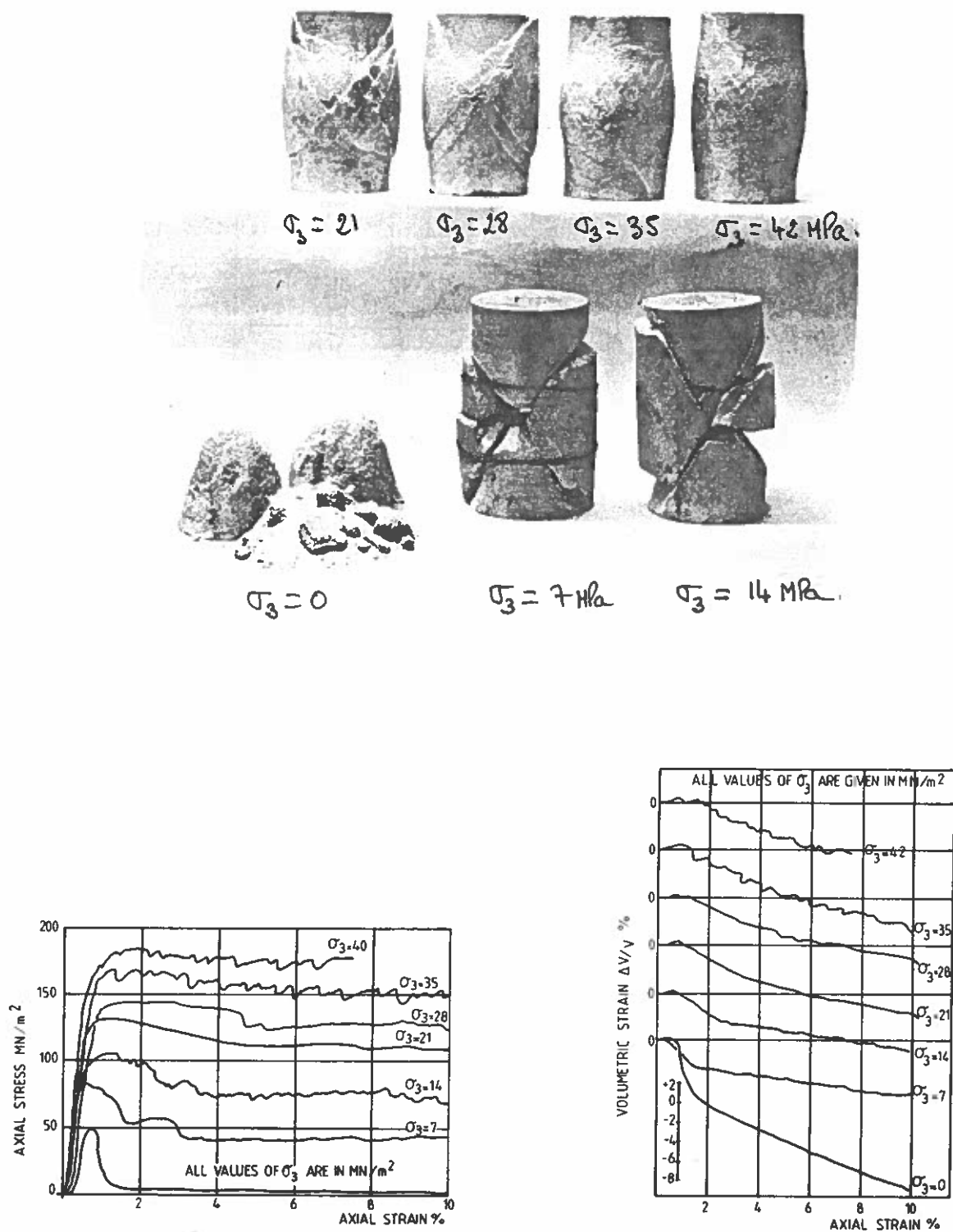


Figure 11. Effect of confinement on fracture strength and rock fracturing. Triaxial tests on saccharoidal limestone (after Farmer, 1983).

## 4. FAILURE CRITERIA FOR INTACT ROCKS AND ROCK MASSES

### 4.1 Mohr Criterion

Mohr (1900) proposed that when shear failure takes place across a plane, the shear and normal stress components  $\tau$  and  $\sigma_n$  acting across that plane are uniquely related as follows

$$|\tau| = f(\sigma_n) \quad (9)$$

Several assumptions are inherent to this criterion:

- Failure takes place when the Mohr circle with radius  $(\sigma_1 - \sigma_3)/2$  is tangent to the Mohr envelope representing equation (9). Failure is assumed to depend only on the major and minor applied principal stresses  $\sigma_1$  and  $\sigma_3$  and is independent on the value of the intermediate principal stress  $\sigma_2$  (Figure 12a).
- Two failure planes develop in a direction parallel to  $\sigma_2$ . The angle between the planes of failure and  $\sigma_1$  increases with  $(\sigma_1 + \sigma_3)/2$ ; this trend has been observed in laboratory tests.
- Tensile and compressive strengths are not equal.

As an example, Figure 12b shows the Mohr circles and the Mohr envelope for 102 tests conducted on Indiana limestone by Robison (1985).

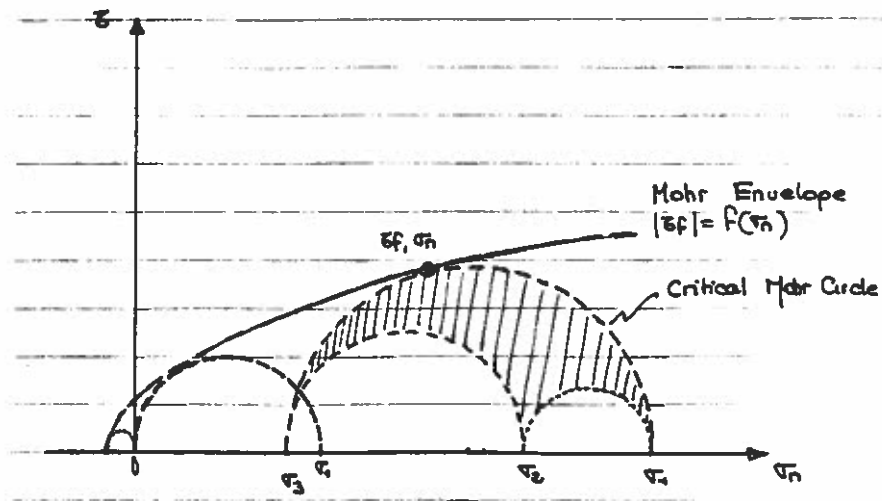
### 4.2 Mohr-Coulomb Criterion

The simplest form of the Mohr envelope is a straight line (Figure 13a) with equation

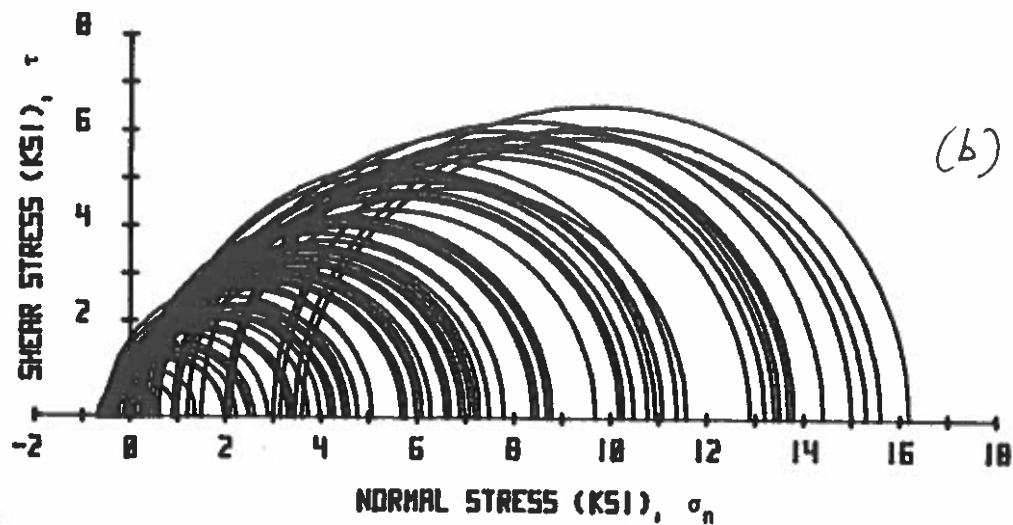
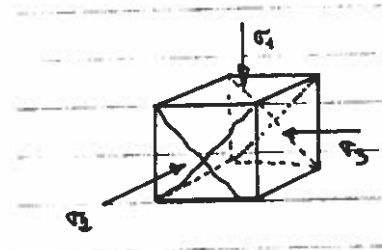
$$|\tau| = S_o + \mu \sigma_n \quad (10)$$

where  $S_o$  is the so-called *inherent shear strength* of the material and  $\mu$  is the so-called *coefficient of internal friction*. The latter is equal to  $\tan \phi$  where  $\phi$  is the so-called *friction angle* by analogy with surface sliding. Values of  $S_o$  and  $\phi$  can be found in Goodman (1989).

According to the Mohr-Coulomb criterion, failure takes place along two conjugate planes inclined at  $\psi_f = \pi/4 - \phi/2$  with respect to the major principal stress,  $\sigma_1$ , and parallel to the intermediate stress  $\sigma_2$ . Also, the orientation of the failure planes does not depend on the stress level.



(a)



(b)

Figure 12. (a) Top half representation of Mohr circles and Mohr envelope, (b) Mohr circles and Mohr envelope for 102 tests on Indiana limestone.

Consider the failure plane shown in Figure 13a and inclined at an angle  $\psi_f$  with respect to  $\sigma_1$ . Using coordinate transformation rules, the normal and shear stresses acting on that plane are equal to

$$\begin{aligned}\sigma_n &= \frac{(\sigma_1 + \sigma_3)}{2} - \frac{(\sigma_1 - \sigma_3)}{2} \sin\phi \\ \tau &= \frac{(\sigma_1 - \sigma_3)}{2} \cos\phi\end{aligned}\tag{11}$$

Substituting the expression of  $\sigma_n$  and  $\tau$  into equation (10), the Mohr-Coulomb criterion can also be expressed in terms of principal stresses as follows

$$\sigma_1 = C_o + \sigma_3 \frac{C_o}{T_o'}\tag{12}$$

with

$$C_o = 2S_o \tan\left(\frac{\pi}{4} + \frac{\phi}{2}\right) ; \quad \frac{C_o}{T_o'} = \tan^2\left(\frac{\pi}{4} + \frac{\phi}{2}\right)\tag{13}$$

Equation (12) has been plotted in Figure 13b. Note that  $T_o'$  is *not* the uniaxial tensile strength of the material since equation (10) implies that, at the time of failure, the normal stress  $\sigma_n$  is positive. It can be shown that this condition implies that  $\sigma_3$  must be larger than  $-T_o'/2$  and  $\sigma_1$  must be larger than  $C_o/2$ . Thus, the two-parameter ( $S_o, \phi$ ) Mohr-Coulomb criterion can be expressed as

$$\begin{aligned}\sigma_1 &= C_o + \sigma_3 \frac{C_o}{T_o'} \quad \text{when } \sigma_1 > C_o/2 \\ \sigma_3 &= -T_o' = -T_o'/2 \quad \text{when } \sigma_1 < C_o/2.\end{aligned}\tag{14}$$

which is represented by two straight lines in Figure 13b. According to the two-parameter criterion, the tensile strength is still related to  $S_o$  and  $\phi$ . The horizontal line  $\sigma_3 = -T_o'$  is called the *tension cutoff*.

A three-parameter Mohr-Coulomb criterion has been proposed. The three parameters include  $S_o$  and  $\phi$  as before and the tensile strength  $T_o$  which is now assumed to be independent of the other

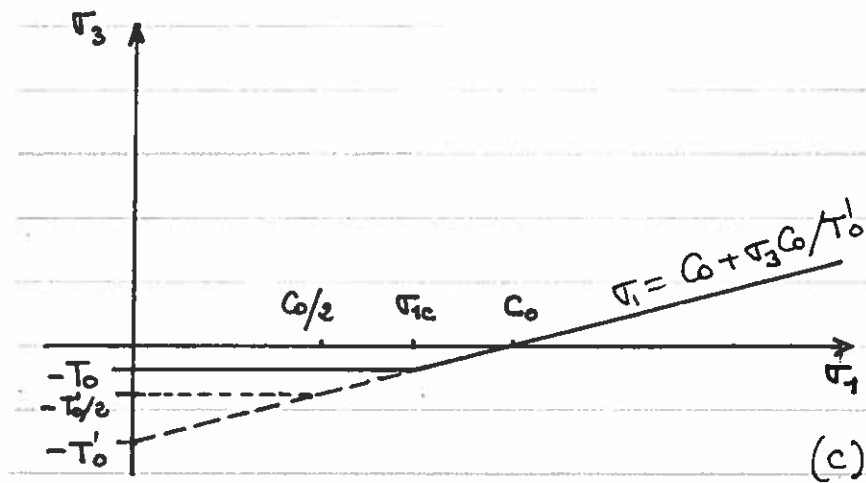
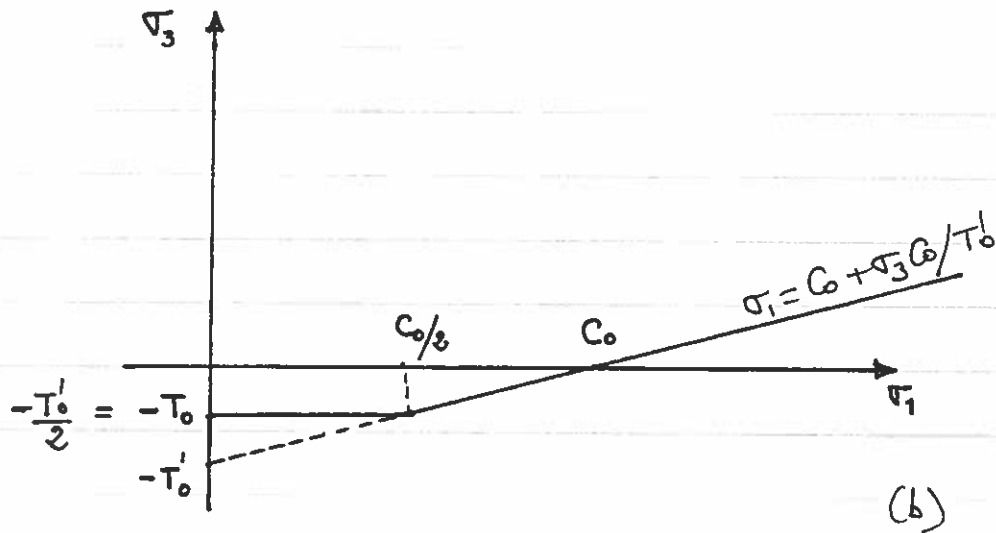
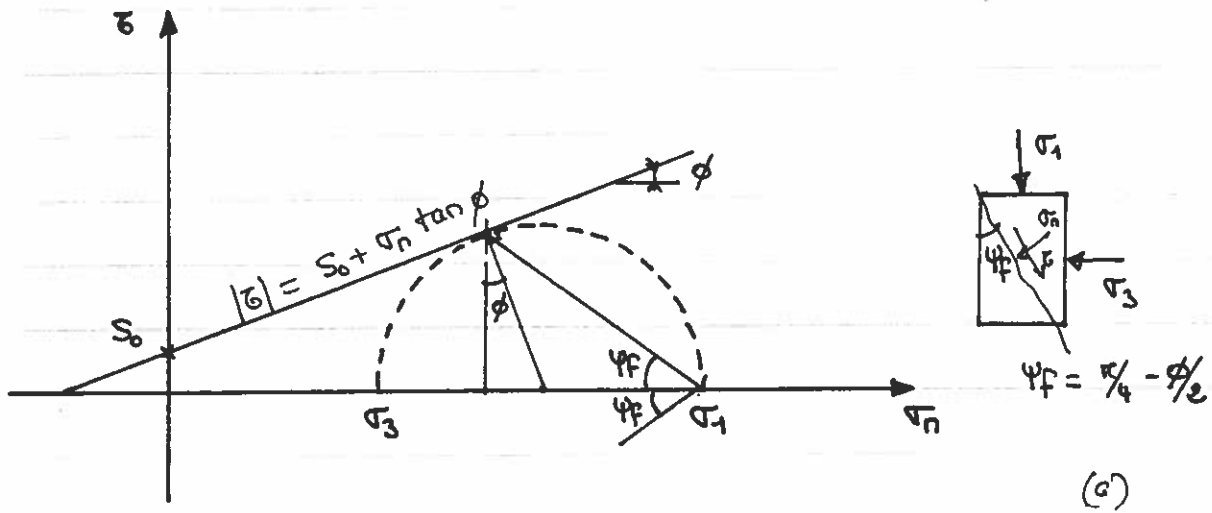


Figure 13. (a) Mohr-Coulomb criterion in the  $(\sigma_n, \tau)$  space, (b) Two-parameter Mohr-Coulomb criterion in  $(\sigma_1, \sigma_3)$  space, (c) Three-parameter Mohr-Coulomb criterion in  $(\sigma_1, \sigma_3)$  space.

two parameters. The criterion is expressed as follows

$$\begin{aligned}\sigma_1 &= C_o + \sigma_3 \frac{C_o}{T_o} \quad \text{when } \sigma_1 > \sigma_{1c} \\ \sigma_3 &= -T_o \quad \text{when } \sigma_1 < \sigma_{1c}\end{aligned}\tag{15}$$

with  $\sigma_{1c} = C_o(1 - T_o/T_o')$ . This criterion is shown in Figure 13c. Note that  $T_o$  must be smaller than  $T_o'/2$  and therefore  $\sigma_{1c}$  must be larger than  $C_o/2$  in order to keep the normal stress across the fracture planes always positive.

Table 3 gives the value of the strength ratio  $C_o/T_o$  when  $\phi = 30^\circ$  for the three cases considered above, i.e. no tension cutoff, two-parameter criterion with tension cutoff, and three-parameter with tension cutoff.

No cutoff $T_o = T_o'$	Two-parameter with cutoff $T_o = T_o'/2$	Three-parameter with cutoff $T_o$ is given
$C_o/T_o = 3$	$C_o/T_o = 6$	$C_o/T_o > 6$

Table 3. Values of the ratio  $C_o/T_o$  for  $\phi = 30^\circ$ .

Figures 14a and 14b show a graphical representation of the three-parameter Mohr-Coulomb criterion in the biaxial plane  $\sigma_z = 0$ , and in the Rendulic plane  $\sigma_x = \sigma_z$ , respectively.

### 4.3 Hoek and Brown Criterion

This is an empirical criterion that does not depend on the intermediate principal stress. It was first proposed by Hoek and Brown (1980b) to model the strength of intact rock and rock masses. In terms of principal stresses, it is expressed as follows

$$\sigma_1 = \sigma_3 + \sqrt{m\sigma_c\sigma_3 + s\sigma_c^2}\tag{16}$$

where

- $\sigma_1$  and  $\sigma_3$  are the major and minor principal stresses at failure,
- $\sigma_c = C_o$  is the uniaxial compressive strength of the intact part of the rock mass, and,
- $m, s$  are constants that depend on the extent to which the rock mass has been broken before being subjected to the principal stresses.  $s = 1$  for intact rock and  $m$  and  $s$  decrease as the rock mass becomes more fractured.

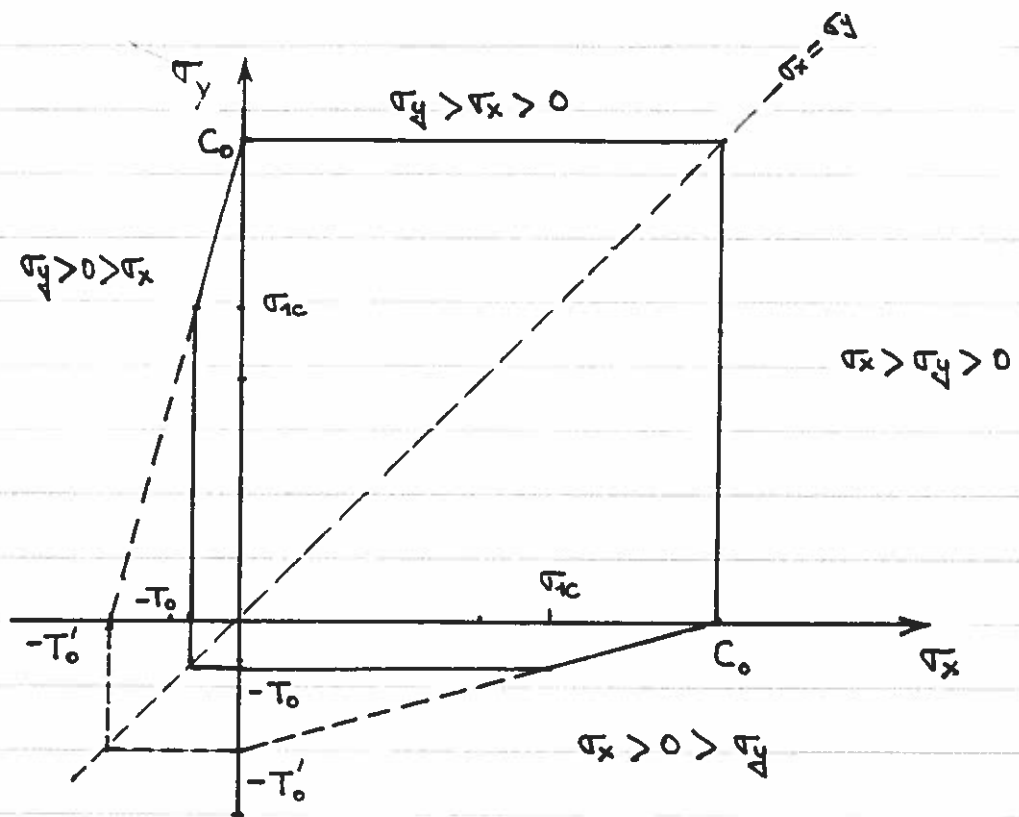
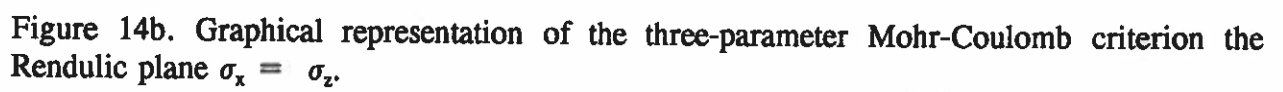


Figure 14a. Graphical representation of the three-parameter Mohr-Coulomb criterion in the biaxial plane  $\sigma_z=0$



The three parameters  $m$ ,  $s$  and  $\sigma_c$  can be determined by regression analysis. The failure criterion is represented in Figure 15a for intact rock. The intact rock tensile strength,  $T_o = \sigma_t$ , predicted by the Hoek and Brown criterion is obtained by setting  $\sigma_1 = 0$  and  $\sigma_3 = -T_o$  in equation (16). This gives,

$$\sigma_t = T_o = \frac{\sigma_c}{2}(\sqrt{m^2 + 4} - m) \quad (17)$$

According to equation (17) the strength ratio  $\sigma_c/\sigma_t$  (or  $C_o/T_o$ ) depends on the value of  $m$  only. For limestone  $m=5.4$  and  $C_o/T_o=5.6$ ; for granite  $m=29.2$  and  $C_o/T_o=29.2$ ; for sandstone  $m=14.3$  and  $C_o/T_o=14.3$ .

The Hoek and Brown criterion for intact rock can also be expressed in terms of normal and shear stresses as follows

$$\tau_n = A(\sigma_n + T_{on})^B \quad (18)$$

with

$$\sigma_n = \sigma/\sigma_c ; \tau_n = \tau/\sigma_c ; T_{on} = T_o/\sigma_c$$

$$\sigma = \sigma_3 + \frac{\tau_m^2}{\tau_m + m\sigma_c/8} \quad (19)$$

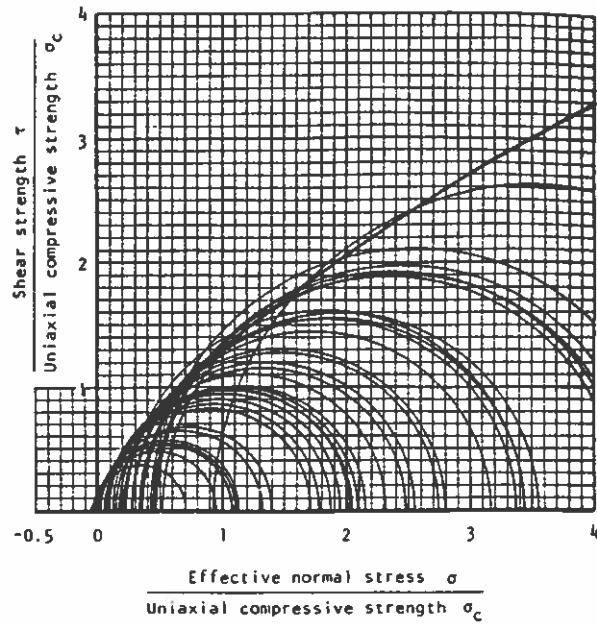
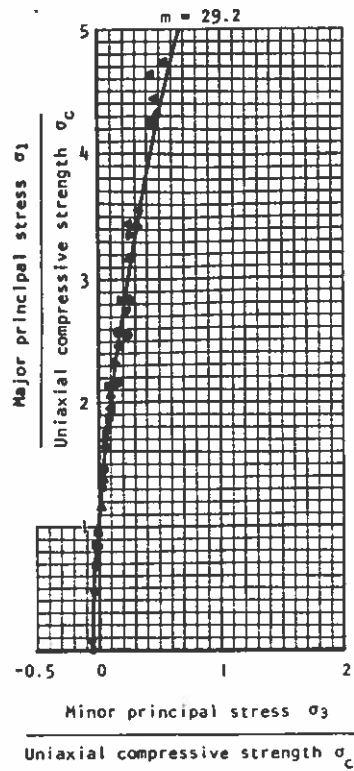
$$\tau = (\sigma - \sigma_3) \sqrt{1 + \frac{m\sigma_c}{4\tau_m}} ; \tau_m = \frac{\sigma_1 - \sigma_3}{2}.$$

In equation (18),  $A$  and  $B$  are found by regression analysis. Equation (17) is the equation of the Mohr envelope in the normal and shear stress space and is represented in Figure 15b. According to the Hoek and Brown criterion, the failure surface is inclined at an angle  $\beta$  to the  $\sigma_1$  axis with  $\sin 2\beta = \tau/\tau_m$ .

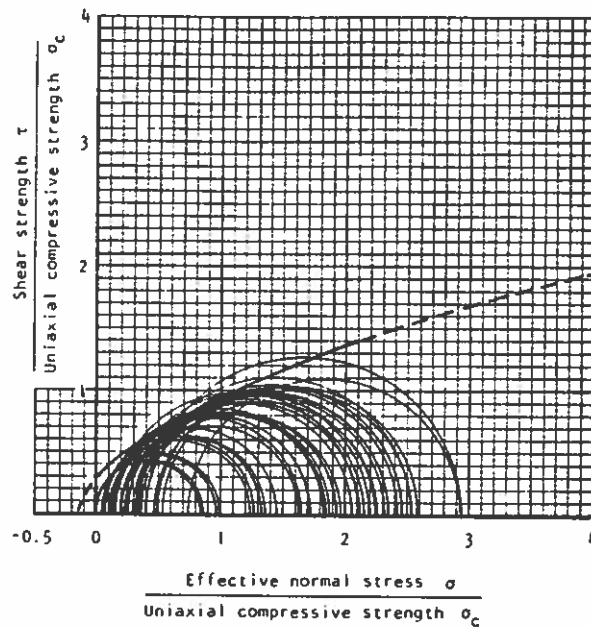
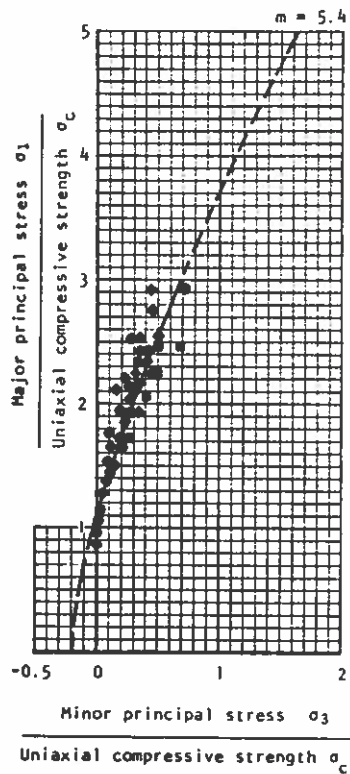
Figure 16 shows typical strength data for granite and limestone analyzed by Hoek and Brown. Values of  $m$  have been proposed for various types of intact rock.

Both the  $m$  and  $s$  coefficients appearing in equation (16) have been related to the RMR and  $Q$  ratings. As discussed by Bieniawski (1993), for intact rock  $m=m_i$  and  $s=1$ . For fractured rock masses,  $m$  and  $s$  are related to the basic (unadjusted) RMR as follows





GRANITE



L I M E S T O N E

Figure 16. Typical data for granite and limestone analyzed by Hoek and Brown (1980a).

Empirical failure criterion $\sigma_1 = \sigma_3 + \sqrt{m\sigma_1\sigma_3 + s\sigma_3^2}$ $\sigma_1$ = major principal effective stress $\sigma_3$ = minor principal effective stress $s$ = uniaxial compressive strength of intact rock and $m$ and $s$ are empirical constants		Carbonate rocks with well-developed crystal cleavage: dolomite, limestone and marble	Lithified argillaceous rocks: mudstone, siltstone, shale and slate (normal to cleavage)	Arenaceous rocks with strong crystals and poorly developed crystal cleavage: sandstone and quartzite	Fine-grained polyminerallic igneous crystalline rocks: andesite, dolerite, diabase and rhyolite	Coarse-grained polyminerallic igneous and metamorphic crystalline rocks: amphibolite, gabbro, gneiss, granite, norite, quartz-diorite
<b>Intact rock samples:</b>						
laboratory size specimens free from discontinuities.		$m^a$	10.00	15.00	17.00	25.00
RMR = 100, Q = 500		$s^a$	1.00	1.00	1.00	1.00
		$m^b$	10.00	15.00	17.00	25.00
		$s^b$	1.00	1.00	1.00	1.00
<b>Very good quality rock mass:</b>						
tightly interlocking.		$m$	3.43	5.14	5.82	8.56
undisturbed rock with unweathered joints at 1-3 m. RMR = 85, Q = 100		$s$	0.082	0.082	0.082	0.082
		$m$	5.85	8.78	9.95	14.63
		$s$	0.189	0.189	0.189	0.189
<b>Good quality rock mass:</b>						
fresh to slightly weathered rock, slightly disturbed with joints at 1-3 m. RMR = 65, Q = 10		$m$	0.821	1.231	1.395	2.052
		$s$	0.00293	0.00293	0.00293	0.00293
		$m$	2.006	4.298	4.871	7.163
		$s$	0.0205	0.0205	0.0205	0.0205
<b>Fair quality rock mass:</b>						
several sets of moderately weathered joints spaced at 0.3-1 m. RMR = 4, Q = 1		$m$	0.183	0.275	0.311	0.458
		$s$	0.00009	0.00009	0.00009	0.00009
		$m$	1.353	2.030	2.301	3.383
		$s$	0.00198	0.00198	0.00198	0.00198
<b>Poor quality rock mass:</b>						
numerous weathered joints at 30-500 mm, some gouge. Clean compacted waste rock. RMR = 23, Q = 0.1		$m$	0.041	0.061	0.069	0.102
		$s$	0.000003	0.000003	0.000003	0.000003
		$m$	0.639	0.959	1.087	1.598
		$s$	0.00019	0.00019	0.00019	0.00019
<b>Very poor quality rock mass:</b>						
numerous heavily weathered joints spaced < 50 mm with gouge. Waste rock with fines. RMR = 3, Q = 0.01		$m$	0.010	0.015	0.017	0.025
		$s$	0.0000001	0.0000001	0.0000001	0.0000001
		$m$	0.313	0.469	0.532	0.782
		$s$	0.00002	0.00002	0.00002	0.00002

<sup>a</sup>First stated  $m$  and  $s$  values are for disturbed rock mass. <sup>b</sup>Second stated  $m$  and  $s$  values are for undisturbed rock mass.

Table 4. Approximate relationship between rock mass quality and material constants (after Bieniawski, 1993).

$$m = m_i \exp[(RMR - 100)/28]$$

$$s = \exp[(RMR - 100)/9]$$
(20)

for smooth-blasted or machine-bored excavations in rock and

$$m = m_i \exp[(RMR - 100)/14]$$

$$s = \exp[(RMR - 100)/6]$$
(21)

for slopes and blast-damaged excavations in rock. Typical values of  $m$  and  $s$  for various rock types and corresponding to various RMR values are listed in Table 4 which is a modified version of that originally proposed by Hoek and Brown (1980a).

Note that the Mohr-Coulomb friction and cohesion can be determined from the Hoek and Brown failure criterion (Hoek, 1990).

### 4.3 Other Failure Criteria

Several other failure criteria that have been used to model the strength of intact rock. A review of those criteria can be found in Jaeger and Cook (1976) and in a recent paper by Lade (1993).

*Kim-Lade Criterion (1984)*

$$\left(\frac{I_1^3}{I_3} - 27\right)\left(\frac{I_1}{p_a}\right)^m = \eta_1$$
(22)

where  $I_1$  and  $I_3$  are the first and third stress invariants,  $\eta_1$  and  $m$  are empirical parameters and  $p_a$  is the atmospheric pressure.

*Druker-Prager Criterion*

$$\sqrt{J_2} = \alpha I_1 + k$$
(23)

where  $\alpha$  and  $k$  are positive material parameters. In terms of octahedral normal and shear stresses, equation (23) becomes

$$\tau_{oct} = C_1 \sigma_{oct} + C_2$$
(24)

The failure surface is a right circular cone in the stress space.

*Criterion of Bresler and Pister (1957)*

$$\tau_{oct}/C_o = f_1(I_1/C_o) + f_2(I_3/C_o^3) \quad (25)$$

where  $C_o$  is the unconfined compressive strength

*Criterion of Murrell (1965)*

$$\sigma_1 = C_o + b\sigma_3^m \quad (26)$$

where  $C_o$ ,  $b$  and  $m$  are constants

*Criterion of Murrell (1963)*

$$(\sigma_x - \sigma_y)^2 + (\sigma_x - \sigma_z)^2 + (\sigma_y - \sigma_z)^2 = 24T_o(\sigma_x + \sigma_y + \sigma_z) \quad (27)$$

or  $J_2 = 4T_o I_1$ . The failure surface is a paraboloid of revolution whose axis is the hydrostatic axis. The paraboloid is terminated by a pyramid formed by the intersection of three planes  $\sigma_x = -T_o$ ,  $\sigma_y = -T_o$ , and  $\sigma_z = -T_o$ .

*Plane Griffith Criterion*

$$\begin{aligned} (\sigma_1 - \sigma_3)^2 &= 8T_o(\sigma_1 + \sigma_3) \quad \text{if } \sigma_1 + 3\sigma_3 > 0 \\ \sigma_3 &= -T_o \quad \text{if } \sigma_1 + 3\sigma_3 < 0 \end{aligned} \quad (28)$$

## 5. REFERENCES

ASTM D 2936-84 Standard test method for direct tensile strength of intact rock core specimen.

ASTM D 2938-86 Standard test method for unconfined compressive strength of intact rock core specimens.

ASTM D 3967-92 Standard test method for splitting tensile strength of intact rock core specimens.

Balmer, G.G. (1953) Physical properties of some typical foundation rocks, *U.S. Bureau of Reclamation Report No. SP-39*.

Bieniawski, Z.T. (1993) Classification of rock masses for engineering: the RMR system and future trends", in *Comprehensive Rock Engineering* (J.A. Hudson ed.), Pergamon, Vol. 3, pp. 553-73.

Bieniawski, Z.T. and Hawkes, I. (1978) Suggested methods for determining tensile strength of rock materials, *Int. J. Rock Mech. Min. Sci. & Geomech. Abstr.*, Vol. 15, No.3, pp. 99-103.

Bieniawski, Z.T. and Bernede, M.J. (coordinators) (1979) Suggested methods for determining the uniaxial compressive strength and deformability of rock materials, *Int. J. Rock Mech. Min. Sci. & Geomech. Abstr.*, Vol. 16, No.2, pp. 135-140.

Broch, E. (1983) Estimation of strength anisotropy using the point load test, *Int. J. Rock Mech. Min. Sci. & Geomech. Abstr.*, Vol. 20, No.4, pp. 181-187.

Broch, E. and Franklin, J.A. (1972) The point load strength test, *Int. J. Rock Mech. Min. Sci.*, Vol. 9, pp. 669-697.

Brown, E.T. (1974) Fracture of rock under uniform biaxial compression, *Proc. 3rd. ISRM Cong.*, Vol. 2, Part A, pp. 111-117.

Farmer, I. (1983) *Engineering Behavior of Rocks*, Chapman and Hall.

Goodman, R.E. (1989) *Introduction to Rock Mechanics*, Wiley, 2nd.Ed.

Hatheway, A.W. and Kiersch, G.A. (1989) Engineering properties of rocks, in *Physical Properties of Rocks and Minerals* (R.S. Carmichael, ed.), CRC Publ., pp. 671-715.

Hoek, E. (1990) Estimating Mohr-Coulomb friction and cohesion values from the Hoek-Brown failure criterion, *Int. J. Rock Mech. Min. Sci. & Geomech. Abstr.*, Vol. 27, No.3, pp. 227-229.

- Hoek, E and Brown, E. T. (1980a) *Underground Excavations in Rock*, Institution of Mining and Metallurgy, London.
- Hoek, E. and Brown, E.T. (1980b) Empirical strength criterion for rock masses. *ASCE J. Geotech. Eng.*, **106**, 1013-1035.
- Jaeger, J.C. and Cook, N.G.W. (1976) *Fundamentals of Rock Mechanics*, Chapman and Hall.
- Johnson, R.B. and DeGraff, J.V. (1988) *Principles of Engineering Geology*, Wiley.
- Lade, P. (1993) Rock strength criteria: the theories and the evidence, in *Comprehensive Rock Engineering* (J.A. Hudson ed.), Pergamon, Vol. 1, pp. 255-284.
- Mogi, K. (1967) Effect of the intermediate principal stress on rock failure, *J. Geophys. Res.*, Vol.72, No.20, pp.5117-5131.
- Mogi, K. (1971) Effect of the triaxial stress system on the failure of dolomite and limestone, *Tectonophysics*, Vol. 11, pp. 11-127.
- Paterson, M.S. (1978) *Experimental Rock Deformation - The Brittle Field*, Springer Verlag.
- Robison, M.J. (1985) The strength of Indiana limestone under multiaxial loading conditions, *MS Thesis*, University of Colorado, Boulder.
- Sture, S. (1973) An improved multiaxial cubical cell and its application to the testing of anisotropic materials, *MS Thesis*, University of Colorado, Boulder.